

# Temperature Control and Noise Reduction in our Compact ADR System for TES Microcalorimeter Operation

U. Hishi<sup>1</sup> · R. Fujimoto<sup>1</sup> · K. Kamiya<sup>1</sup> ·  
M. Kotake<sup>1</sup> · H. Ito<sup>1</sup> · T. Kaido<sup>1</sup> · K. Tanaka<sup>1</sup> ·  
K. Hattori<sup>1</sup>

Received: 30 September 2015 / Accepted: 2 March 2016 / Published online: 22 March 2016  
© Springer Science+Business Media New York 2016

**Abstract** We have been developing a compact adiabatic demagnetization refrigerator, keeping ground application and future missions in mind. A salt pill fabricated in-house, a superconducting magnet with a passive magnetic shield around it, and a mechanical heat switch are mounted in a dedicated helium cryostat. The detector stage temperature is regulated by PID control of the magnet current, with a  $dI/dt$  term added to compensate the temperature rise due to parasitic heat. The temperature fluctuation of the detector stage is  $1\text{--}2\ \mu\text{K}_{\text{rms}}$ , and the hold time was extended by about 15% thanks to the  $dI/dt$  term. Bundle shields of the harnesses between the cryostat and the analog electronics boxes were connected to the chassis at both ends, and the analog electronics boxes were grounded to the cryostat through the bundle shields. This reduced the readout noise to  $16\ \text{pA}/\sqrt{\text{Hz}}$  in the 10–60 kHz range. Using this system, an energy resolution of  $3.8 \pm 0.2\ \text{eV}$  (FWHM) was achieved at 5.9 keV.

**Keywords** Adiabatic demagnetization refrigerator · TES microcalorimeter · PID control

## 1 Introduction

An X-ray microcalorimeter measures the energy of an X-ray photon as a temperature rise [1]. It achieves very high spectroscopic performance of  $E/\Delta E > 1000$  at 6 keV, when operated at  $<0.1\ \text{K}$ . More importantly, its performance does not degrade even if an object is extended. The soft X-ray spectrometer (SXS) onboard ASTRO-H,

---

✉ U. Hishi  
hishi@astro.s.kanazawa-u.ac.jp

<sup>1</sup> Division of Mathematical and Physical Sciences, Graduate School of Natural Science and Technology, Kanazawa University, Kakuma-machi, Kanazawa, Ishikawa 920-1192, Japan

which will be launched in early 2016, utilizes a thermistor-type microcalorimeter array [2]. A transition edge sensor (TES)-type microcalorimeter array will be adopted by future missions such as DIOS [3]. To operate an X-ray microcalorimeter in orbit, a cooling system that works under zero gravity is needed. An adiabatic demagnetization refrigerator (ADR) is one of the most practical solutions. Since a TES and a SQUID readout are sensitive to the magnetic fields, we think it is important to develop a detector and a readout together with an ADR. Therefore, we are developing a compact ADR and a TES microcalorimeter as one system, keeping ground application and future use in orbit in mind.

In our previous paper [4], we reported that the transition edge was degraded due to the magnetic field of the ADR, and it was improved by introducing a proper magnetic shield around the superconducting magnet. The energy resolution was 15 eV (FWHM) at 5.9 keV. In this paper, we report the temperature control and the noise reduction, and the improvement of the detector performance is measured in our ADR system.

## 2 Our ADR System

Our ADR system is composed of a single-stage salt pill made of ferric ammonium alum (FAA), and pumped liquid helium as the heat sink. In a dedicated He cryostat, a salt pill is mounted with a superconducting magnet and a conventional mechanical heat switch on a liquid He temperature stage. The He temperature stage is protected by a He temperature shield and two layers of vapor-cooled shields and multi-layer insulation (MLI). Its cross section is shown in Fig. 1. A block diagram and grounding configuration of the cryostat and the electronics boxes is shown in Fig. 2. Details of its design are shown elsewhere [5].

The lowest accessible temperature is below 40 mK, the hold time at 100 mK is over 21 h when demagnetization starts at 1.8 K, and parasitic heat load to the detector stage is 1–3  $\mu$ W. To shield magnetic field of the ADR, we attached a 12-mm-thick silicon steel (ferromagnetic) shield around the superconducting magnet. Magnetic field at the detector position is reduced to below geomagnetic field by this shield even when 3 T field is applied during ADR recycling. The detector is shielded by a combination of an aluminum (superconductor) shield inside and a Cryoperm (ferromagnetic) shield outside. The SQUID readout is shielded by a combination of a niobium (superconductor) shield inside and a Cryoperm shield outside, and is located on the He temperature stage.

## 3 System Improvement

### 3.1 Temperature Control

To keep the detector temperature constant, we control the magnet current with a proportional–integral–derivative (PID) controller method. The temperature of the detector stage is monitored with a ruthenium oxide thermometer (Lakeshore, RX202A), and it is read by a cryogenic temperature controller Cryo-con Model 62,

once per second. The parameters are determined using the ultimate gain method. The temperature fluctuation in our system is 1–2  $\mu\text{K}$  rms at 75 mK.

In case of ADR operation, a conventional PID method is not sufficient, since it is needed to decrease the magnet current to compensate parasitic heat, even if there is no temperature fluctuation. If we use a conventional PID method, a temperature offset is needed to reduce the magnet current with the proportional term and the integral term. In order to make the PID control work properly, a term that represents current decrease is needed [6]. Hereafter, we call it a  $dI/dt$  term. We calculate the  $dI/dt$  term using two points that are 300 s apart. Each of them was averaged for 100 s. We compared temperature controls at 75 mK, with and without a  $dI/dt$  term. The results are shown in Fig. 3. By introducing the  $dI/dt$  term, the temperature drift originally seen at the last part of the hold time, where the current decrease rate became larger, was significantly suppressed, and the hold time was extended by about 15 %. We verified its repeatability, and concluded that it is not due to a change in the experimental setup but to the change of the control loop, though the reason is not understood yet. The temperature fluctuation was, on the other hand, unchanged.

When we read out the temperature using Cryo-con Model 62, built-in filtering capability is enabled to reduce readout noise. The results shown above are obtained using the filter time constant of 16 s. This means, however, the PID terms are calculated after integration for 16 s. We compared the temperature fluctuation by changing the filter time constant. At that time, we increased the excitation voltage from 333  $\mu\text{V}$  to 1 mV to reduce readout noise. The temperature fluctuation was  $\sim 3$  and  $\sim 10$   $\mu\text{K}$  rms with the filter time constant of 4 and 1 s, respectively. In the former case, the energy resolution was unchanged, while in the latter case, the temperature reading

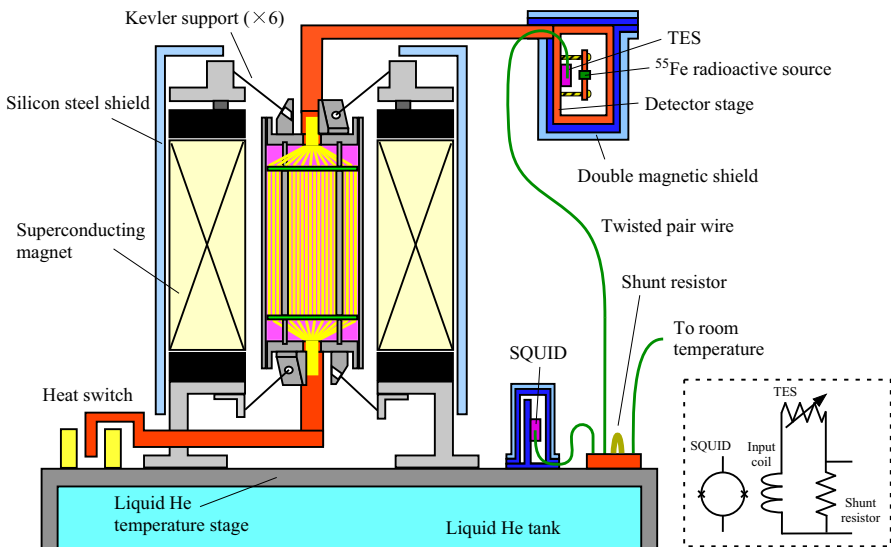


**Fig. 1** The cross section of our ADR system. The inset shows a circuit diagram of the detector and the SQUID readout (Color figure online)

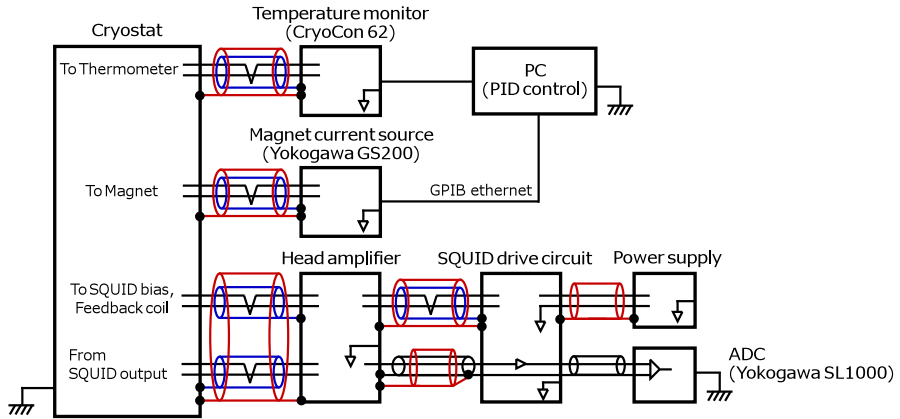


**Fig. 2** Configuration diagram of the cryostat and the electronics boxes with their grounding and harness shielding, after modification described in Sect. 3.2 (Color figure online)

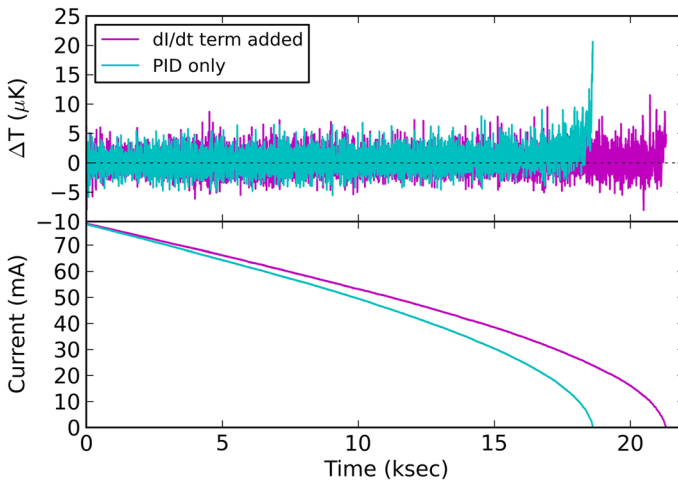


**Fig. 3** Temperature residuals and magnet currents as a function of time, with and without a  $dI/dt$  term (Color figure online)

was noisy and we could not properly introduce the D term. Note that the temperature reading changed from 75 to 81 mK, by increasing the excitation voltage. Therefore, the temperature was controlled at 81 mK at that time. The noise power has the largest contribution at 0.02–0.06 Hz and at around 0.1 Hz, when the filter time constant is 16 and 4 s, respectively. Noise in the higher frequency range is suppressed when a longer filter time constant is selected.

### 3.2 Noise Environment

Hishi et al. [4] reported that proper shielding of superconducting magnets is critical to achieve a sharp transition edge. The energy resolution of the TES was, however,

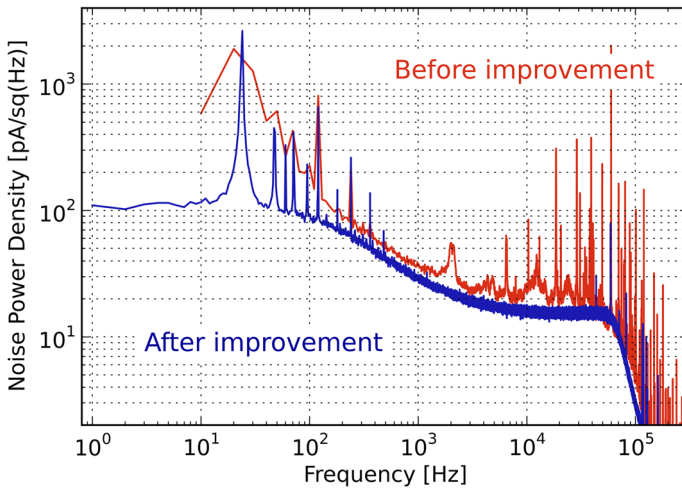


**Fig. 4** Noise power spectra before and after the changes. They were measured at 4.2 K, when the detector was not operated. They are dominated by the readout noise, since the level of the Johnson noise is only  $\sim 3 \text{ pA}/\sqrt{\text{Hz}}$ . Note that the 26 Hz noise and its harmonics are caused by the SQUID drive circuit that we are using (Color figure online)

15 eV, even though a detector that has an intrinsic resolution of 5.7 eV was used. Accordingly, we further tried to reduce noise. First, we replaced the analog-to-digital converter module that has 12 bit resolution with that has 16 bit resolution, in order to reduce quantization noise. Second, we thoroughly implemented the following principles of harness shielding and grounding: (1) to use shielded twisted-pair cables with bundle shields between the cryostat and the analog electronics boxes (a SQUID drive and readout circuit, a bias current supply to the TES, a current supply to the superconducting magnet); (2) connect both ends of the bundle shields to the chassis to construct a Faraday cage; and (3) connect the individual shields to the chassis only at the signal output side. The analog electronics boxes were grounded to the cryostat through the bundle shields. See Fig. 2 for the configuration of the grounding and the harness shielding.

Noise spectra before and after these changes, obtained when the detector temperature was 4.2 K which is dominated by the readout noise, are shown in Fig. 4. The continuum level in the frequency range between 10 and 60 kHz was improved from 22 to 16  $\text{pA}/\sqrt{\text{Hz}}$ , and features above 1 kHz were significantly suppressed. The energy resolution at 5.9 keV was improved to 6.6 eV.

#### 4 Spectroscopic Performance

We evaluated the spectroscopic performance in our ADR system using a TES microcalorimeter that has 2.7 eV resolution at 5.9 keV [7]. The detector was operated at 75 mK and at the resistance of 0.13 times the normal resistance. An optimal filter was applied to each pulse record to calculate its pulse height. The energy scale was corrected with a quadratic polynomial, using Mn  $K\alpha/K\beta$  peaks and the origin. Pulse

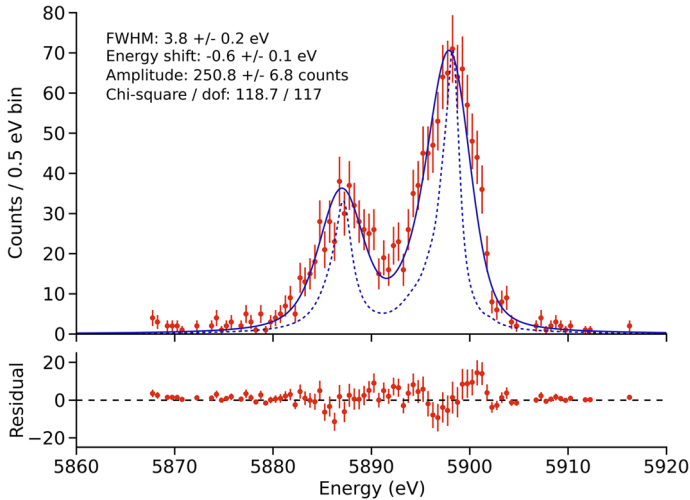


**Fig. 5** Pulse height spectrum of Mn  $K\alpha$  photons (Color figure online)

height drift was corrected by using the DC level offset just before the arrival of the pulse. An energy spectrum thus obtained is shown in Fig. 5. The energy resolution was  $3.8 \pm 0.2$  eV (FWHM).

This is worse than the intrinsic resolution of the detector we used, indicating that there still exists an additional noise term that has 2.8 eV contribution in our ADR system. When we applied the same optimal filter to the noise records obtained at 4.2 K, the width of the pulse height peak distribution was 2.7 eV. This suggests that the energy resolution measured in our ADR system is limited mainly by the readout noise, especially by the hump seen in the frequency range below 10 kHz.

## 5 Summary

We are developing a compact ADR for TES microcalorimeter operation. The detector temperature is regulated by controlling the magnet current with a PID method. Temperature fluctuation is 1–2  $\mu\text{K}$  rms, with 16 s filter time constant of the readout electronics, while it is  $\sim 3$   $\mu\text{K}$  rms if the filter time constant is 4 s and higher excitation voltage is selected. By introducing a  $dI/dt$  term, to compensate the temperature increase due to parasitic heat load, the hold time was extended by about 15%. Shielding and grounding of the entire system were reinvestigated, and bundle shields of the harnesses between the cryostat and the analog electronics boxes were connected to the chassis at both ends to construct a Faraday cage, and analog electronics boxes were grounded to the cryostat through the bundle shields. This reduced the readout noise from 22 to 16  $\text{pA}/\sqrt{\text{Hz}}$  in the 10–60 kHz frequency range. The energy resolution was improved to  $3.8 \pm 0.2$  eV (FWHM) at 5.9 keV by these measures. It is suggested that it is limited by the hump of the readout noise in the frequency range below 10 kHz.

## References

1. S.H. Moseley, J.C. Mather, D. McCammon, *J. Appl. Phys* **56**, 1257 (1984)
2. K. Mitsuda et al., *Proc. SPIE* **9144**, 91442A (2014)
3. T. Ohashi et al., *Proc. SPIE* **9144**, 91442Q (2014)
4. U. Hishi et al., *J. Low Temp Phys.* **176**, 1075 (2014)
5. A. Hoshino et al., *J Low Temp. Phys.* **167**, 554–560 (2012)
6. A. Hoshino et al., *MIMA* **558**, 536 (2006)
7. H. Akamatsu et al., *AIP Conf. Proc.* **1185**, 195 (2009)